The Numerical Investigation of Flow-Induced Sound Generation from a Simplified Alternator Geometry

Matthew Wasko, Martin Fischer

Robert Bosch GmbH, Corporate Research, Department of Applied Physics, Acoustics (CR/ARP3), D-70049 Stuttgart, Germany

Email: Matthew.Wasko@de.bosch.com; Martin.Fischer7@de.bosch.com

Introduction

This investigation describes a numerical study of the flow-induced noise generating mechanisms of a simplified, alternator-based geometry. This geometry is designed such that it includes the components that have an impact on the fluid flow and acoustic field of a real alternator geometry. Subsequently we use the surface pressure fluctuations determined from an unsteady RANS (Reynolds-Averaged Navier-Stokes) fluid dynamics solution as input into a code based on Lowson's method for rotating acoustic sources. We compare the solution to experimental results obtained in a semi-anechoic chamber from an equivalent physical model.

Acoustic Sources

Aeroacoustic sources acting on a system can be grouped into three major types: Quadrupole, dipole and monopole sources. In the case of subsonic, industrial rotating machinery with thin blade geometry, only the dipole source term is considered as a significant source [1,2,3]. This source term is related to both steady and unsteady pressures experienced by the solid surfaces with respect to a stationary observer.

For machinery producing subsonic flows that undergo velocity fluctuations at the surfaces, the sound source is predominantly due to the fluctuating pressure components, as shown in Equation (1) [4]. Here, n is a multiple of the rotational frequency, U_0 is the speed of the moving dipole, w is the order of magnitude of the inflow velocity variations (i.e. upwash at the blade) and M_0 is the Mach number of the moving dipole.

$$\frac{\text{Steady Loading Noise}}{\text{Unsteady Loading Noise}} = \frac{1}{n^2}\left(\frac{U_0}{w}\right)^2\left(\frac{M_0}{1-M_0}\right)^2 \qquad (1)$$

Figure 1 shows a numerical analysis by the authors comparing the steady and unsteady loading cases at a speed of 10,000 rpm revealing the dominance of the unsteady loading noise term. This is particularly the case for high harmonics and moderate to high local velocity fluctuations. For industrial machines, moderate to high harmonics are of interest due to their audible nature, while significant local velocity fluctuations are expected due to upstream disturbances from stationary geometry (i.e. struts).

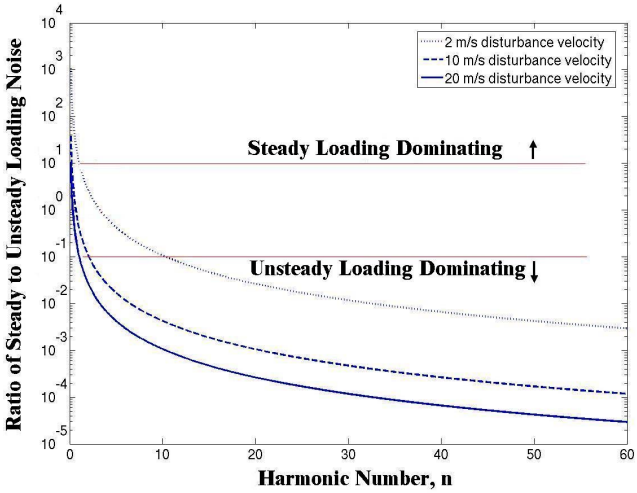

Figure 1: An analysis of the dominance of unsteady loading noise at 10,000 rpm for various disturbance velocities. Even for small disturbance velocities, much of the higher harmonics are largely dependant on the unsteady loading on the surfaces. A value of 1 indicates equal importance from both source types.

Computational Modeling

In order to capture the significant effects due to the aforementioned unsteady loading, transient fluid dynamics simulations must be conducted. A simple geometry, see Figure 2, was designed with key components that were modified at various stages of the research. The model comprises of several rotating and stationary surfaces which correspond to surfaces in real alternator geometries.

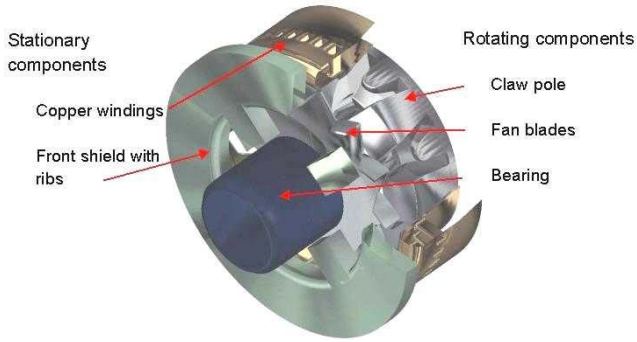

Figure 2: Example of the geometries tested. The stationary and rotating components produce the major mechanisms of aeroacoustic noise present in actual alternator geometries.

Fluid Dynamics

We use the commercial package Ansys CFX and employ a hexahedral grid consisting of approximately 1.4 million cells and model only a quarter of the model. Initial steady state results were obtained using an SST (Shear Stress Transport) RANS turbulence model. Interfaces between rotating and stationary domains consist of both frozen rotor (in regions of high circumferential flow change) and stage interfaces. The time averaged solutions were then used as an initial input for a transient simulation, where two full revolutions were computed. The SST model was also used in the transient simulations, with fully transient domain interfaces implemented between the rotating and stationary assemblies.

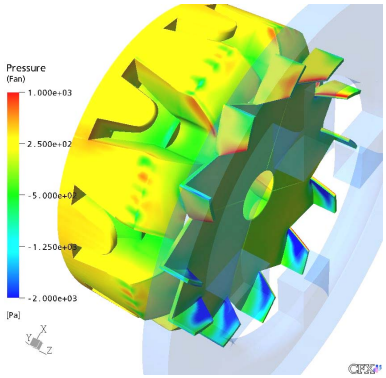

Figure 3: Surface pressures across the rotating surfaces at a single time step. Fluctuations on the blades and claw poles are particularly evident.

The results obtained from these transient simulations, a single time step shown in Figure 3, provide evidence of the location of sound sources, indicated by regions of high fluctuations. Pressure fluctuations were evident in the rotating components; high fluctuations were noted on the fan blades, due to the disturbance initiated by the upstream struts, in addition to fluctuations at several claw pole locations, due to the interaction with the fan blades as well as the outer casing, particularly in the region of the casing holes.

Aeroacoustics

The aeroacoustic problem can be solved using the Ffowcs-Williams and Hawkings (FWH) equation, a wave equation with source terms derived from the aerodynamic conservation of mass and momentum equations. Considering only dipole sources in an arbitrary motion, Lowson's formulation solves the FWH equation in the frequency domain, see Equation 2 [1,2]. Here, c_n is the nth complex frequency magnitude, $2\pi/\omega$ is the time for one full period, r is the distance between source and microphone, F_r is the surface force in the direction of the microphone, a_0 is the speed of sound and τ is the retarded time.

$$c_n = \frac{-\omega}{4\pi^2 r} \int_0^{2\pi/\omega} \left(\frac{in\omega F_r}{a_0} \right) e^{in\omega\left(\tau + r/a_0\right)} d\tau \qquad (2)$$

The aeroacoustic code developed by the authors allows the import of any rotating surface into the formulation and allows calculation of the total power integral over a specified set of microphones, in addition to determining the individual surface contributions. In order to compare to the experimental procedure, ISO 3745 standards were adopted. Influences from the stationary components were ignored, as was the reflective plane present during experiments.

In the test case shown in Figure 4, results from only one blade and one clawpole were imported. Harmonics that experimentally were the most significant were predicted well. Poor prediction of the 8th harmonic (1333 Hz) is noted, possibly due to a lack in force data needed in order to predict low frequencies accurately. Each harmonic has various contributions from the surfaces; claw pole surfaces contribute to every 8th harmonic (every 1333 Hz), fan blade surfaces to every 12th (every 2000 Hz). The total power level was underpredicted by 0.45 dB, in other tested cases deviations of up to about 3 dB were observed.

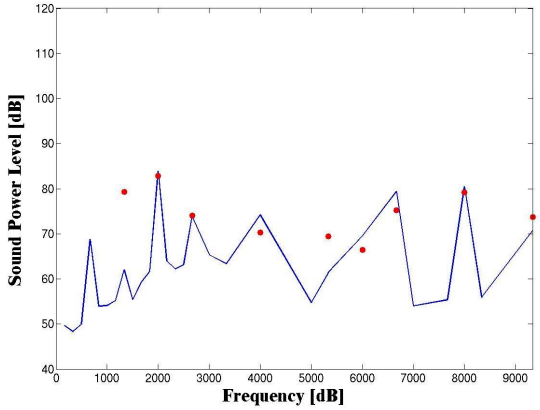

Figure 4: Total power levels obtained numerically (points) compared to an equivalent experimental case (line).

Conclusion

Initial results using the aeroacoustic code demonstrate good consistency between experimental results. The major harmonics are predicted well, as is the total power level. This suggests good modeling of the sources at the rotating surfaces. Further work will be conducted on the modeling of ground surfaces, in order to more closely represent the experimental conditions, in addition to modeling the stationary surfaces of the geometry, such as the casing.

References

[1] M.V. Lowson, The sound field for singularities in motion. Proceedings of the Royal Society of London **286** (1965), 559-572

[2] M.V. Lowson, Theoretical analysis of compressor noise. The Journal of the Acoustical Society of America **47(1)** (1970), 371-385

[3] W. Neise, Review of fan noise generation mechanisms and control methods. Fan Noise: An International INCE Symposium (1992), 45-46

[4] M. Roger, Noise from moving surfaces. Advances in Aeroacoustics and Applications Lecture Series (2004)